

**A Peroxisome Proliferator-activated Receptor- $\gamma$  (PPAR $\gamma$ ) agonist, Troglitazone, facilitates caspase-8 and -9 activities by increasing the enzymatic activity of Protein Tyrosine Phosphatase-1B on human glioma cells**

Yasuharu Akasaki, Gentao Liu, Harry H. Matundan, Hiushan Ng, Xiangpeng Yuan, Zhaohui Zeng, Keith L. Black & John S. Yu

From Maxine Dunitz Neurosurgical Institute, Cedars-Sinai Medical Center, Los Angeles, California 90048

Running title: Facilitation of caspase activity by a PPAR $\gamma$  agonist

Address correspondence to: John S. Yu, Maxine Dunitz Neurosurgical Institute, Cedars-Sinai Medical Center, Suite 800 East, 8631 West 3<sup>rd</sup> Street, Los Angeles, California 90048, Phone: (310) 423-0875, Fax: (310) 423-0810; E-mail: [yuj@cshs.org](mailto:yuj@cshs.org)

Despite dramatic advances in adjuvant therapies, patients with malignant glioma face a bleak prognosis. Since many adjuvant therapies seek to induce glioma apoptosis, strategies that lower thresholds for the induction of apoptosis may improve patient outcomes. Therefore, elucidation of the biological mechanisms that underlie resistance to current therapies is needed to develop new therapeutic strategies. Here, we propose a novel mechanism of pro-apoptotic effect induced by a pharmacological Peroxisome Proliferator-activated Receptor- $\gamma$  (PPAR $\gamma$ ) agonist, Troglitazone, that facilitates caspase signaling in human glioma cells. Troglitazone activates Protein Tyrosine Phosphatase (PTP)-1B, which subsequently reduces phospho-tyrosine-705 STAT3 (pY705-STAT3) via a PPAR $\gamma$ -independent pathway. Reduction of pY705-STAT3 in glioma cells caused down-regulation of FLICE-inhibitory protein (FLIP) and Bcl-2. Furthermore, Troglitazone induced Serine-392-phosphorylation of p53 via a PPAR $\gamma$ -dependent pathway and up-regulation of Bax in a p53-wild-type glioma. When given with TRAIL or caspase-dependent chemotherapeutic agents, such as Etoposide and Paclitaxel, Troglitazone exhibited a synergistic effect by facilitating caspase-8/9 activities. A PPAR $\gamma$  antagonist, GW9662, did not block this effect, although a PTP inhibitor (PTPI) abrogated it. Knockdown of STAT3 by STAT3-siRNA negated the inhibitory effect of PTPI on Troglitazone, indicating that Troglitazone uses a

STAT3-inactivation mechanism that makes caspase-8/9 activities susceptible to cytotoxic agents in glioma cells, and that PTP1B plays a critical role in the down-regulation of activated-STAT3, as well as FLIP and Bcl-2. When taken with caspase-dependent anti-neoplastic agents, Troglitazone may be a promising drug for use against malignant gliomas because it facilitates the caspase cascade, thereby lowering thresholds for the apoptosis induction of glioma cells.

Malignant gliomas adopt the ability to bypass or disrupt failsafe mechanisms, such as programmed cell death and host immune defense (1-3), which make current therapeutic interventions ineffective at eradicating residual tumor reservoirs. Since many adjuvant therapies for malignant tumors seek to induce tumor cell apoptosis, strategies that lower thresholds for the induction of apoptosis, which can then make other treatments more effective, may improve patient outcomes. Therefore, further understanding of the biological anti-apoptotic mechanisms that govern resistance to conventional glioma therapies is required in order to develop safer and more effective treatments.

Tumor necrosis factor-related apoptosis-inducing ligand (TRAIL) is a promising anti-neoplastic agent because it induces apoptosis in cancer cells with only negligible effect on normal cells (4,5). It has been known that TRAIL triggers caspase cascade through interaction with TRAIL-responsive death receptors (DR), such as DR4 and DR5, which induce

cleavage of caspase-8 in the Fas-associated death domain protein (FADD)-dependent mechanism (6). In this pathway, cleaved caspase-8 plays a significant role as an initiator that can process other members in the caspase cascade. Cleaved caspase-8 induces cleavage of Bid, which up-regulates mitochondrial cytochrome c (Cyt-c) release (7). Then the Cyt-c cooperates with Apaf-1 to activate caspase-9 (8). After these activations, both caspase-8 and -9 activate caspase-3, which is the primary activator of apoptotic DNA fragmentation, and leads to cancer cell apoptosis (9).

Despite the numerous reports describing the favorable anti-tumor activities of TRAIL, malignant gliomas exhibit considerable heterogeneity in their sensitivity to TRAIL, even among those expressing DR4 and DR5 (5,10). In this regard, it has recently been reported that several cancers, including gliomas, constitutively express FADD-like IL-1 $\beta$ -converting enzyme (FLICE)-inhibitory protein (FLIP) (11-13), which is a cytoplasmic protein that inhibits the recruitment and processing of caspase-8 (12), and that the overexpression of FLIP induces cancer's resistance to DR-dependent apoptosis (14). In addition, it has also been found that Bcl-2 family proteins modulate caspase-9 activity by controlling the permeability of mitochondrial membranes, and that dysregulation of these proteins in cancer cells correlates with their anti-apoptotic potential and progression (15). Specifically, the anti-apoptotic Bcl-2 family, including Bcl-2 and Bcl-xL, stabilize the mitochondrial porin channel (VDAC) and inhibit Cyt-c release (16), whereas the pro-apoptotic Bcl-2 family, including Bax and Bad, antagonize this process by competitive heterodimerization with anti-apoptotic Bcl-2 proteins (17). Although down-regulation of FLIP and/or anti-apoptotic Bcl-2 family proteins are therefore a therapeutic target for promotion of caspase cascade activity, the mechanism that regulates these proteins in glioma cells is not fully understood.

In this report, we demonstrate that a

Peroxisome Proliferator-activated Receptor- $\gamma$  (PPAR $\gamma$ ) agonist, Troglitazone, facilitates caspase-8 and -9 actions by down-regulating FLIP and Bcl-2 in human glioma cells. Troglitazone induces inactivation of Signal Transducer and Activator of Transcription-3 (STAT3), and synergistically enhances the cytotoxic effects of TRAIL and other caspase-dependent chemotherapeutic drugs. This effect is exhibited through a PPAR $\gamma$ -independent mechanism, in which Protein Tyrosine Phosphatase 1B (PTP1B) plays a critical role in the down-regulation of activated-STAT3, as well as FLIP and Bcl-2. Here we propose a novel mechanism to explain the pro-apoptotic effect induced by Troglitazone in human glioma cells.

### Experimental procedure

*Tumor cells.* A human primary cultured glioma (MG-328) was established from the surgical specimen of a patient with newly diagnosed glioblastoma at Cedars-Sinai Medical Center after IRB-approved consent was obtained. MG-328 and human glioma cell lines, U-87MG (American Type Culture Collection, Rockville, MD) and LN-18 (provided by Dr. Erwin Van Meier, Emory University, GA) were maintained at 37°C and 5% CO<sub>2</sub> in DMEM/F-12 with 10% heat-inactivated FBS, 2 mM glutamate, 10 mM HEPES, 100 U/ml penicillin, and 100  $\mu$ g/ml streptomycin.

*Reagents.* Recombinant human TNF-related apoptosis inducing ligand (rTRAIL) was obtained from Pepro Tech (Rocky Hill, NJ). A PPAR $\gamma$  agonist, Troglitazone (TG), was obtained from BIOMOL International (Plymouth Meeting, PA). A PPAR $\gamma$  antagonist, GW9662 (GW), was obtained from Cyman Chemical (Ann Arbor, MI). Protein tyrosine phosphatase (PTP)-inhibitor (PTPI),  $\alpha$ -Bromo-4-hydroxyacetophenone, and Src homology 2 (SH2) containing PTP (SHP)-inhibitor (SHPI),  $\alpha$ -Bromo-4-carboxymethoxyacetophenone, were obtained from CALBIOCHEM (San Diego, CA). Etoposide (VP16) and Paclitaxel

(Taxol) were obtained from Sigma-Aldrich (St. Louis, MO). TG, GW, PTPI, SHPI, VP16, and Taxol were dissolved in 100% DMSO as 1000x stock solution and then diluted further in culture medium. Cells were treated with rTRAIL (17.5~300 ng/ml), TG (30  $\mu$ M), GW (20  $\mu$ M), PTPI (50  $\mu$ M), SHPI (200  $\mu$ M), VP16 (0.01~10  $\mu$ M), and/or Taxol (0.005~5  $\mu$ M).

*siRNA design and transfection.* A double-stranded siRNA oligonucleotide against STAT3 was designed as follows and as previously described (18): 5'-AAC AUC UGC CUA GAU CGG CUA dTdT-3'; 3'-dTdT GUA GAC GGA UCU AGG CGA U-5' (STAT3-siRNA; Dharmacon RNA Technologies, Lafayette, CO). siRNA for non-silencing control (non-silencing siRNA) is an irrelevant siRNA with random nucleotides and no known specificity. Sequences were synthesized and annealed by the manufacturer (Qiagen, Valencia, CA) as previously described (19). STAT3-siRNA (50-600 pmol) or non-silencing siRNA (600 pmol) was transfected to glioma cells ( $1 \times 10^6$  cells) with Oligofectamine Reagent (Invitrogen Life Technologies, Carlsbad, CA) according to the manufacturer's protocol, and the cells were used for experiments 24h after transfection.

*RNA isolation and cDNA synthesis.* Total RNA was extracted from glioma cells ( $1 \times 10^6$  cells) using the RNA4PCR kit (Amibion, Austin, TX) according to the manufacturer's protocol. For cDNA synthesis, 1  $\mu$ g total RNA was reverse-transcribed into cDNA using Oligo dT primer and iScript™ cDNA Synthesis Kit reverse transcriptase. cDNA was stored at  $-20^\circ\text{C}$  for PCR.

*Real-time Quantitative RT-PCR.* Gene expression was quantified by real-time quantitative RT-PCR using QuantiTect SYRB Green dye (Qiagen, Valencia, CA). DNA amplification was performed using an Icyler (BIO-RAD, Hercules, CA), and the binding of the fluorescence dye SYBR Green I to double-stranded DNA was measured. The

PCR reactions were set up in microtubes in a volume of 25  $\mu$ l. Oligonucleotide primers were designed as follows: STAT3 forward, 5'-GCC AGA GAG CCA GGA GCA-3', STAT3 reverse, 5'-ACA CAG ATA AAC TTG GTC TTC AGG TAT G-3', and  $\beta$ -actin forward, 5'-TTC TAC AAT GAG CTG CGT GTG-3',  $\beta$ -actin reverse, 5'-GGG GTG TTG AAG GTC TCA AA-3'. The reaction components were 2.0  $\mu$ g of cDNA synthesized as above, 12.5  $\mu$ l of 2 $\times$  QuantiTect SYRB Green PCR Master Mix (Qiagen, Valencia, CA), and 0.4  $\mu$ M of each pair of oligonucleotide primers. The program was as follows: initial activation for 15 min at  $95^\circ\text{C}$ , 50 cycles consisting of melting for 30 sec at  $95^\circ\text{C}$ , annealing for 25 sec at  $60^\circ\text{C}$ , and extension for 30 sec at  $72^\circ\text{C}$ . After cycling, relative quantification of target gene mRNA against an internal control, beta-actin, was possible by the following a  $\Delta C_T$  method and an amplification plot of fluorescence signal vs. cycle number was drawn. The difference ( $\Delta C_T$ ) between the mean values in duplicated samples of the target gene and those of beta-actin was calculated using Microsoft Excel and the relative quantification value (RQV) was expressed as  $2^{-\Delta C_T}$ . The relative expression of each sample in the figure was normalized by "No treatment" expression.

*Abs.* Rabbit polyclonal Abs against DR4, DR5 and PPAR $\gamma$  were obtained from Cyman Chemical. Mouse monoclonal Abs against STAT3, phospho-tyrosine-705 STAT3 (pY705-STAT3), which is an activated form of STAT3, Bax and Bcl-2 were obtained from BD Pharmingen (San Diego, CA). Rabbit polyclonal Abs against p53 and phospho-Ser392-p53 (pS392-p53) were obtained from Cell Signaling Technology (Beverly, MA). Mouse monoclonal Abs against PTP1B (PTPase1B; AE4-2J) and SH2-containing PTP-1 (SHP1; 1SH01), and rabbit polyclonal Ab against FLIP were obtained from CALBIOCHEM. Mouse monoclonal Ab of  $\beta$ -tubulin was

obtained from Sigma-Aldrich. HRP-linked Abs of sheep anti-mouse IgG and donkey anti-rabbit IgG were obtained from Amersham Biosciences (Piscataway, NJ).

**Western blot.** Samples were extracted with buffer containing 1% Triton X-100, 150 mM NaCl, 50 mM Tris (pH 7.5) and 1 mM PMSF (Roche, Indianapolis, IN), and were subjected to SDS-PAGE with 30 $\mu$ g general protein loading into each lane on a 10% polyacrylamide gel. Electrophoretic transfer to nitrocellulose membranes (Amersham Bioscience) was followed by immunoblotting. The signal was detected using an ECL detection system (Amersham Bioscience).

**Apoptosis assay and cell viability assay.** Treatment of cells with TG, GW, PTPI and/or SHPI for 24h was followed by treatment with rTRAIL (VP16 or Taxol), and all the cells, including cells that had not adhered, were harvested after 24h (48h). An Annexin V-FITC apoptosis detection kit I (BD Pharmingen) was used for viability assay of the cells. Cells were stained with Annexin V-FITC (Ann) and Propidium Iodide (PI) according to the manufacturer's protocol, and were analyzed by FACS (BD pharmingen). Cells that stained negative for both Ann and PI were defined as viable cells for viability assay.

**Caspase activity assay.** Activity of caspase-3, -8 and -9 were measured using Caspase-3/ CPP32, FLICE/Caspase-8, and APOPCYTO/Caspase-9 Colorimetric Assay Kits, respectively, from Medical and Biological Laboratories Co. (Nagoya, Japan). Briefly, the treatment of cells with TG, GW and/or PTPI for 24h was followed by treatment with rTRAIL (VP16 or Taxol). After 2h (24h) of treatment, all the cells were harvested and samples were extracted with Cell Lysis Buffer. Concurrently, a sample for a negative control was extracted from the cells without apoptosis induction. A standard curve using the absorbance of *p*-nitroanilide standards was constructed, and then the specific activities on each sample were calculated according to the manufacturer's protocol.

**Statistics.** Student's T test was used for statistical comparison of results.

## Results

**The role of STAT3 in resistance to TRAIL-induced apoptosis.** To examine the mechanism that causes resistance to TRAIL, we used glioma cell lines that are partially resistant to TRAIL despite their expression of DR4 and/or DR5. Western blot was used to detect the expression levels of DR4 and DR5 in LN-18, U-87MG and MG-328 (Figure 1A). The cytotoxic activity of TRAIL (18.75-300 ng/ml) was examined in each glioma (Figure 1B, C). As shown in Figure 1B, which is a representative result of FACS analysis using an Annexin-V apoptosis detection kit on LN-18, treatment with TRAIL (300 ng/ml) increased the percentage of Ann(+)/PI(-) cells, which indicates early stage of apoptosis, after 2h-treatment (33.7%) and 24h-treatment (60.1%) compared with no treatment control (2.2%). Treatment with 300 ng/ml of TRAIL induced 40-60% cell death after 24h-treatment (Figure 1C), although the viable cells maintained a proliferative ability after 72h cell-culture with 300 ng/ml TRAIL (not shown). These findings indicate that these gliomas can acquire a resistance to TRAIL despite their expression of functionally intact DR4/5.

After this observation, we sought to determine whether STAT3 contributes to the gliomas' resistance to TRAIL using STAT3-specific small interference RNA (STAT3-siRNA) (18). The specificity of STAT3-inhibition in LN-18 after transfection with STAT3-siRNA was investigated by real-time quantitative PCR and Western blot analysis (Figure 2A, B). Although neither non-silencing control or vehicle control had any significant change in expressions of STAT3-mRNA or STAT3-protein compared with the no treatment control, STAT3-siRNA transfection in glioma cells decreased both STAT3-mRNA (Figure 2A) and STAT3-protein (Figure 2B) expressions in a dose-dependent manner. These findings indicate that the STAT3-siRNA used in this study exhibited a STAT3-specific silencing

effect. As shown in Figure 2B and 2C, Western blot analysis detected high levels of STAT3, pY705-STAT3, FLIP and Bcl-2 in the no treatment control, non-silencing control, and vehicle control. The pY705-STAT3 was down-regulated concomitant with the decrease in STAT3 in STAT3-siRNA-transfected glioma cells (Figure 2B, C). In addition, FLIP and Bcl-2 expression levels decreased in the STAT3-siRNA groups (Figure 2B, C), suggesting that knockdown of STAT3 induces down-regulation of FLIP and Bcl-2 in glioma cells by inhibiting the transcriptional activity of STAT3. Bax expression levels, which is a pro-apoptotic protein induced by p53, were not altered by knockdown of STAT3 (Figure 2B, C). To further confirm the regulatory function of STAT3 on the DR-signaling pathway, the non-silencing control, vehicle control and STAT3-siRNA-transfected cells were treated with 100 ng/ml TRAIL, and then cell viability (Figure 2D) and caspase activity assays (Figure 2E) were performed. Transfection of STAT3-siRNA to glioma cells did not induce their apoptotic death, but it significantly enhanced TRAIL's cytotoxic effect (Figure 2D). The specific activities of caspases-3, -8 and -9 were also significantly increased in the siRNA-transfected group (Figure 2E). In the assessment of the 72h cell-culture, TRAIL (100 ng/ml) killed more than 95% of the cells in the siRNA-transfected group of each glioma (not shown). These results indicate that STAT3 plays a critical role in these gliomas' resistance to TRAIL. Down-regulation of FLIP and Bcl-2 in the STAT3-siRNA-transfected group may have a particular relevance to the facilitation of the activity of caspase-3, -8 and -9.

*Troglitazone activities via PPAR $\gamma$ -dependent and -independent pathways.* We sought to determine whether a PPAR $\gamma$  agonist would enhance TRAIL-induced apoptosis. Using a Western blot analysis, PPAR $\gamma$  expression was observed in LN-18 and U-87, but not in

MG-328 (Figure 3A). Treatment over 48h with Troglitazone (TG), which is a pharmacological PPAR $\gamma$  agonist, did not induce apoptotic death on glioma cells but did significantly enhance the cytotoxic activity of TRAIL not only in LN-18 and U-87MG but also in MG-328 (Figure 3B). These results suggest the possibility that the synergistic effect of TG on TRAIL is controlled by a PPAR $\gamma$ -independent mechanism. Although TG had no effect on STAT3 expression levels, it induced down-regulation of pY705-STAT3 (Figure 3C). In addition, TG diminished FLIP and Bcl-2 protein expression in these cells (Figure 3C), which was probably caused by down-regulation of pY705-STAT3. TG-treatment in U-87MG, of which p53 is a wild type (20), increased Bax expression levels, although Bax levels were not altered in LN-18, which is a p53 mutant cell line (20), or in MG-328 (Figure 3C). Although we did not confirm the sequence of p53 in MG-328, this result may indicate that TG up-regulates a transcriptional activity of p53 via a PPAR $\gamma$ -dependent pathway, in which wild-type-p53 should induce up-regulation of Bax.

Next, we used a PPAR $\gamma$  antagonist, GW9662 (GW), to clarify the role of PPAR $\gamma$  in TG's effect on these glioma cells. Similar to the effect of TG alone, down-regulation of pY705-STAT3 was observed on the cells treated with TG and GW (Figure 4A), indicating that the inhibitory effect of TG on pY705-STAT3 is caused via a PPAR $\gamma$ -independent pathway.

In a previous report, it was demonstrated that phosphorylation of p53 at Serine-392 (pS392-p53) influenced the growth suppressor function and transcriptional activation of p53 (21). Based on this report, we confirmed the expression levels of pS392-p53 as an index of the transcriptional activity of p53. As shown in Figure 4A, GW abrogated the up-regulation of pS392-p53 induced by TG in LN-18 and U-87MG. GW also inhibited the up-regulation of Bax found in TG-treated U-87MG. There was no

significant change in the expression levels of pS392-p53 or Bax in MG-328 in either setting (Figure 4A). These results indicate that TG induces phosphorylation of p53 at Serine-392 via a PPAR $\gamma$ -dependent pathway, and causes up-regulation of Bax in gliomas that have a wild-type-p53. Although these results suggest that TG may have the potential to control caspase cascade signaling via both PPAR $\gamma$ -dependent and -independent pathways, the synergistic activity of TG in TRAIL-treated glioma cells was not blocked by a PPAR $\gamma$  antagonist even in U-87MG, as assessed by a cell viability assay (Figure 4B). In addition, treatment with GW did not reduce the specific activities in any caspases that we observed (Figure 4C), indicating that the synergism of TG in TRAIL-treated glioma cells occurs through a PPAR $\gamma$ -independent mechanism. Taken together, these results indicate that inactivation of STAT3 and the subsequent down-regulation of the downstream proteins, such as FLIP and Bcl-2, by TG may have a particular relevance to the mechanism by which TG synergistically enhances TRAIL's pro-apoptotic effect.

*The significance of PTP1B activity in TG's effect.* PTP1B negatively regulates tyrosine phosphorylation of JAK2 and STAT3 (22,23). In addition, SHP-1 negatively regulates STAT3 activity by facilitating tyrosine dephosphorylation of the upstream JAK2 (24). Based on these findings, we hypothesized that the inhibitory effect of TG on pY705-STAT3 may be caused by activation of these PTP proteins. To confirm the relationship between pY705-STAT3 and PTPs, protein samples extracted at different time points after treatment with TG were subjected to Western blot in which pY705-STAT3, PTP1B and SHP-1 expression levels were analyzed (Figure 5). In this assay, up-regulation of the activated form of PTP1B (42 kDa), which is induced by a proteolysis of 50 kDa PTP1B (25,26), was thought to start within 4h after TG treatment, and its expression reached maximum levels in 16-32h in all of these

gliomas. On the other hand, down-regulation of pY705-STAT3 was noticeable at 8h, and its expression continued to decrease after 8h until 32h. SHP-1 was constitutively and highly expressed in all of these gliomas, and TG had only a negligible effect on SHP-1 expression.

To confirm the role of PTP activity in the mechanism controlling TG's synergistic effect on TRAIL-treated glioma cells, we used  $\alpha$ -Bromo-4-hydroxyacetophenone (PTPI), which is an inhibitor for both PTP1B and SHP-1, and  $\alpha$ -Bromo-4-carboxymethoxyacetophenone (SHPI), which is a specific inhibitor for SHP-1 (27). Specifically, TG-treated glioma cells were co-treated with PTPI or SHPI, and then were assessed by Western blot, and by cell viability and caspase activity assays. In the Western blot analysis, PTPI abrogated the inhibitory effect of TG on pY705-STAT3 (Figure 6A), whereas SHPI did not inhibit the down-regulation of pY705-STAT3 induced by TG (Figure 6B). These findings indicate that activation of PTP1B, but not SHP-1, is involved in the inhibitory effect of TG on pY705-STAT3. PTPI did not inhibit the up-regulation of pS392-p53 in LN-18 and U-87MG caused by TG. Neither STAT3 nor p53 expression levels were altered in either setting (Figure 6A). In the cell viability (not shown) and caspase activity assays (Figure 6C), PTPI abrogated the synergistic effect of TG on TRAIL, although SHPI did not abrogate it (not shown). Thus, these results indicate that PTP1B plays a critical role in TG's effect that enhances the cytotoxic activity of TRAIL in glioma cells.

Furthermore, we sought to determine whether STAT3-inactivation is a key target for PTP1B in this mechanism. To confirm this, STAT3-siRNA transfected glioma cells were treated with TG, PTPI and TRAIL, and were then subjected to caspase activity assay. In this assessment, the inhibitory effect of PTPI on TG was negated in the STAT3-siRNA transfected glioma cells (Figure 6D). These results indicate that activation of PTP1B by means of proteolysis of 50 kDa PTP1B and the subsequent

tyrosine dephosphorylation of pY705-STAT3 is a key mechanism in this effect.

*The synergism of TG with chemotherapeutic drugs.* Given the already described ability of TG to facilitate caspase cascade in glioma cells by attenuating FLIP and Bcl-2 expression levels, TG may also exhibit a synergistic effect with chemotherapeutic drugs that activate caspase-8 and -9. Based on this hypothesis, we sought to determine whether TG enhances the cytotoxic activities of Etoposide (VP16) and Paclitaxel (Taxol), which are known to involve activation of caspase-2,-8,-9 and -10 during their apoptosis induction (28-30). To confirm this, treatment of U-87MG with TG and/or PTPI was followed by treatment with VP16 (0.01-10  $\mu$ M) or Taxol (0.005-5  $\mu$ M). The cells were then subjected to cell viability (Figure 7A, B) and caspase activity assays (Figure 7C, D). The synergistic activities of TG for both VP16 (Figure 7A, C) and Taxol (Figure 7B, D) were observed in all of the assays. Although PTPI had only a limited effect in inhibiting cytotoxic (Figure 7A, B) and caspase-3 activity (Figure 7C, D) in these assessments, PTPI completely abrogated the effect of TG on the activity of caspase-8 and -9 (Figure 7C, D). These results indicate that TG uses a specific mechanism that makes caspase-8 and -9 activities susceptible to cytotoxic agents in glioma cells, and that PTP1B plays a critical role in the down-regulation of constitutively activated STAT3, as well as the downstream FLIP and Bcl-2 in this mechanism. Although the exact reason for the limited inhibitory effect of PTPI on cytotoxic or caspase-3 activity was not determined, these results suggest that TG may have other pro-apoptotic activities that are exhibited through a caspase-3-dependent and PTP1B-independent mechanism.

Further observation of the 5-day cell-cultures in these assessments found that more than 95% of the cells in the TG- and TG/PTPI-treatment groups were killed by VP16 (10  $\mu$ M) or Taxol (5  $\mu$ M), whereas the cells in the control group maintained an ability to proliferate (not shown). Therefore, TG may be a promising drug that can

abrogate the mechanism that makes malignant gliomas resistant to cytotoxic agents.

Based on these results, we schematized the synergistic activities of TG in the caspase cascade (Figure 8). Specifically, TG induces activation of PTP1B and the subsequent tyrosine dephosphorylation of constitutively activated STAT3 in glioma cells via a PPAR $\gamma$ -independent pathway. This event causes down-regulation of FLIP and Bcl-2, and facilitates the activities of caspase-8 and -9 when taken with caspase-dependent anti-neoplastic agents. TG also has the ability to induce transcriptional activation of p53 via a PPAR $\gamma$ -dependent pathway. In the cells with wild-type-p53, this event causes up-regulation of Bax, which can facilitate caspase-9 activity, although this may be only a minor effect of the synergism with TG. Thus, TG enhances the cytotoxic effect of caspase-dependent anti-neoplastic agents, such as TRAIL, VP16 and Taxol, by facilitating caspase cascade signaling in glioma cells. PTP1B plays a critical role in this mechanism.

## Discussion

PPAR $\gamma$  is a member of the nuclear hormone receptor superfamily of ligand-activated transcription factors. Interaction of PPAR $\gamma$  with its agonists, such as 15-deoxy-delta<sup>12,14</sup>-Prostaglandin J<sub>2</sub> (15dPGJ<sub>2</sub>) and Thiazolidenediones (TZD), exerts anti-tumor effects in a variety of cancers, indicating anti-proliferative, anti-angiogenic and pro-differentiation effects (31). Apart from these anti-tumor activities, contradictory evidence in support of the tumor-promoting activity of PPAR $\gamma$  has been observed in Min mice, with a genetic predisposition to adenomatous polyposis coli (32,33). Thus, the question of whether PPAR $\gamma$  is a tumor suppressor gene remains controversial. Despite the oncogenic activities of PPAR $\gamma$ , it is now recognized that PPAR $\gamma$  agonists have pro-apoptotic activities, and many of them are induced through PPAR $\gamma$ -independent pathways (31).

Therefore, PPAR $\gamma$ -independent mechanisms triggered by PPAR $\gamma$  agonists may have particular relevance to the paradoxical findings on the effect of PPAR $\gamma$  in cancer cells, although the mechanisms are not fully understood. Among the PPAR $\gamma$ -independent effects, PPAR $\gamma$  agonists mediate pro-apoptotic and anti-inflammatory activities by inhibiting the transcriptional activities of the STAT family, including STAT1, 3 and 5 (34-36). Furthermore, it has been recently reported that the pro-apoptotic activity of a PPAR $\gamma$  agonist acting via a PPAR $\gamma$ -independent mechanism correlates with the inhibitory effect on FLIP and Bcl-xL/Bcl-2 functions (37,38).

It has been shown that activated STAT3 contributes to the inhibition of Fas-mediated apoptosis signaling by affecting the expression levels of FLIP and Bcl-2 (39). Activation (i.e. tyrosine phosphorylation) of STAT3 is induced by signaling through JAK/STAT-associated receptors such as gp130, growth hormone receptors, interferon receptors, and Receptor Tyrosine Kinases (RTK), of which gp130, exemplified by the IL-6 receptor, and RTKs, exemplified by EGFR and VEGFR, have been reported as key mediators in the inappropriate activation of STAT3 in glioma cells (40-42). In our studies, STAT3 in glioma cells was constitutively activated, and FLIP and Bcl-2 were highly expressed. Knockdown of STAT3 by its specific siRNA facilitated caspase cascade signaling by attenuating FLIP and Bcl-2 expression. Furthermore, this effect was faithfully reproduced by a PPAR $\gamma$  agonist, Troglitazone, which induced down-regulation of pY705-STAT3, FLIP and Bcl-2 in glioma cells via a PPAR $\gamma$ -independent pathway.

It is well established that tyrosine phosphorylation is negatively regulated by PTPs, which represent a large and structurally diverse family of enzymes that rivals the protein tyrosine kinases (PTK) family, including RTKs, in structural diversity and complexity (43,44). PTKs, PTPs and their corresponding substrates are

integrated within elaborate signal transducing networks, in which PTPs can either antagonize or potentiate PTK-induced signaling events *in vivo*. Defective or inappropriate operation of these networks leads to aberrant tyrosine phosphorylation, which contributes to the development of many human diseases including cancers (45). So far, RTK activity and the effect of RTK inhibitors on malignant glioma have been noted (46,47), but the role of PTPs in gliomas is largely unknown.

In our report, expression levels of the cytoplasmic non-transmembrane PTP family, PTP1B and SHP-1, were analyzed after treatment with Troglitazone. Expression levels of 42 kDa PTP1B, which is an activated form of PTP1B implicated as a negative regulator in multiple RTK signaling pathways (43), were extremely low in glioma cells, and Troglitazone induced proteolysis of 50 kDa PTP1B to 42 kDa proteins. On the other hand, SHP-1, which negatively regulates STAT3 activity by facilitating tyrosine dephosphorylation of the upstream JAK2 on the gp130 receptor (24), was constitutively and highly expressed in all these gliomas, and Troglitazone had only a negligible effect on SHP-1 expression. In the experiment using covalent inhibitors for PTP and SHP, a PTP inhibitor abrogated the effect of Troglitazone on glioma cells. Furthermore, knockdown of STAT3 by STAT3-siRNA negated the inhibitory effect of a PTP inhibitor on Troglitazone, indicating that Troglitazone uses a STAT3-inactivation mechanism that makes caspase-8 and -9 activities susceptible to cytotoxic agents in glioma cells, and that PTP1B plays a critical role in the inhibitory effect on the signaling pathway through inappropriately activated JAK/STAT3 receptors in glioma cells.

The pharmacological mechanism by which Troglitazone activates PTP1B remains unknown. PTP1B was initially described as a 37 kDa protein with tyrosine-specific protein phosphatase activity. Subsequent studies demonstrated that this purified protein represented a truncated form of a 50 kDa enzyme that is associated with the

endoplasmic reticulum through interaction of its C-terminus with the cytoplasmic face (25). Cleavage of the C-terminus of PTP1B by intracellular  $\text{Ca}^{2+}$  influx and subsequent calpain activation correlates with the appearance of a 42 kDa protein, increased PTP1B enzymatic activity and release from the endoplasmic reticulum (26,48). A more recent study suggests that  $\text{Ca}^{2+}$  release-activated  $\text{Ca}^{2+}$  influx is inhibited by tyrosine dephosphorylation and that PTP1B plays a critical role in this dephosphorylation process (49). Palakurthi and colleagues demonstrated that TZD induces intracellular  $\text{Ca}^{2+}$  release via a PPAR $\gamma$ -independent mechanism (50). Based on these findings, it is likely that depletion of intracellular  $\text{Ca}^{2+}$  stores by TZD treatment triggers activation of an intracellular  $\text{Ca}^{2+}$  influx in the cells exhibiting low PTP1B enzymatic activity. Therefore,  $\text{Ca}^{2+}$  release-activated  $\text{Ca}^{2+}$  influx and subsequent calpain activation may be a critical mechanism by which Troglitazone activates PTP1B in glioma cells via a

PPAR $\gamma$ -independent pathway.

Here, we demonstrated that inactivation of constitutively activated STAT3 concomitant with PTP1B activation plays a critical role in the synergistic effect of Troglitazone on the cytotoxic activities of anti-neoplastic agents in glioma cells. Although Troglitazone may have the ability to facilitate caspase-3 activity and other pro-apoptotic signals through a PTP1B-independent pathway, we note that Troglitazone is a promising anti-neoplastic agent due to its synergistic ability to facilitate caspase-8 and -9 signaling in a PTP1B-dependent manner. These findings support the possibly enhanced effectiveness of using PPAR $\gamma$  agonists in clinical chemotherapy protocols that also use caspase-dependent anti-neoplastic agents such as TRAIL, Etoposide and Paclitaxel for patients with malignant tumors as a means of facilitating the caspase cascade.

### References

1. Chakravarti, A., Zhai, G. G., Zhang, M., Malhotra, R., Latham, D. E., Delaney, M. A., Robe, P., Nestler, U., Song, Q., and Loeffler, J. (2004) *Oncogene* **23**, 7494-7506
2. Bobola, M. S., Emond, M. J., Blank, A., Meade, E. H., Kolstoe, D. D., Berger, M. S., Rostomily, R. C., Silbergeld, D. L., Spence, A. M., and Silber, J. R. (2004) *Clin Cancer Res* **10**, 7875-7883
3. Akasaki, Y., Liu, G., Chung, N. H., Ehtesham, M., Black, K. L., and Yu, J. S. (2004) *J Immunol* **173**, 4352-4359
4. Ashkenazi, A., Pai, R. C., Fong, S., Leung, S., Lawrence, D. A., Marsters, S. A., Blackie, C., Chang, L., McMurtrey, A. E., Hebert, A., DeForge, L., Koumenis, I. L., Lewis, D., Harris, L., Bussiere, J., Koeppen, H., Shahrokhi, Z., and Schwall, R. H. (1999) *J Clin Invest* **104**, 155-162
5. Hao, C., Beguinot, F., Condorelli, G., Trencia, A., Van Meir, E. G., Yong, V. W., Parney, I. F., Roa, W. H., and Petruk, K. C. (2001) *Cancer Res* **61**, 1162-1170
6. Thomas, L. R., Henson, A., Reed, J. C., Salsbury, F. R., and Thorburn, A. (2004) *J Biol Chem* **279**, 32780-32785
7. Kuwana, T., Smith, J. J., Muzio, M., Dixit, V., Newmeyer, D. D., and Kornbluth, S. (1998) *J Biol Chem* **273**, 16589-16594
8. Li, P., Nijhawan, D., Budihardjo, I., Srinivasula, S. M., Ahmad, M., Alnemri, E. S., and Wang, X. (1997) *Cell* **91**, 479-489
9. Wolf, B. B., Schuler, M., Echeverri, F., and Green, D. R. (1999) *J Biol Chem* **274**, 30651-30656
10. Knight, M. J., Riffkin, C. D., Muscat, A. M., Ashley, D. M., and Hawkins, C. J. (2001) *Oncogene* **20**, 5789-5798
11. Yoon, G., Kim, K. O., Lee, J., Kwon, D., Shin, J. S., Kim, S. J., and Choi, I. H. (2002) *J Neurooncol* **60**, 135-141

12. Krueger, A., Baumann, S., Krammer, P. H., and Kirchhoff, S. (2001) *Mol Cell Biol* **21**, 8247-8254
13. Zhang, X., Jin, T. G., Yang, H., DeWolf, W. C., Khosravi-Far, R., and Olumi, A. F. (2004) *Cancer Res* **64**, 7086-7091
14. Rippo, M. R., Moretti, S., Vescovi, S., Tomasetti, M., Orecchia, S., Amici, G., Catalano, A., and Procopio, A. (2004) *Oncogene* **23**, 7753-7760
15. Reed, J. C. (1999) *Curr Opin Oncol* **11**, 68-75
16. Shimizu, S., Narita, M., and Tsujimoto, Y. (1999) *Nature* **399**, 483-487
17. Adams, J. M., and Cory, S. (1998) *Science* **281**, 1322-1326
18. Konnikova, L., Kotecki, M., Kruger, M. M., and Cochran, B. H. (2003) *BMC Cancer* **3**, 23
19. Liu, G., Ng, H., Akasaki, Y., Yuan, X., Ehtesham, M., Yin, D., Black, K. L., and Yu, J. S. (2004) *Eur J Immunol* **34**, 1680-1687
20. Van Meir, E. G., Kikuchi, T., Tada, M., Li, H., Diserens, A. C., Wojcik, B. E., Huang, H. J., Friedmann, T., de Tribolet, N., and Cavenee, W. K. (1994) *Cancer Res* **54**, 649-652
21. Kohn, K. W. (1999) *Mol Biol Cell* **10**, 2703-2734
22. Zabolotny, J. M., Bence-Hanulec, K. K., Stricker-Krongrad, A., Haj, F., Wang, Y., Minokoshi, Y., Kim, Y. B., Elmquist, J. K., Tartaglia, L. A., Kahn, B. B., and Neel, B. G. (2002) *Dev Cell* **2**, 489-495
23. Kaszubska, W., Falls, H. D., Schaefer, V. G., Haasch, D., Frost, L., Hessler, P., Kroeger, P. E., White, D. W., Jirousek, M. R., and Trevillyan, J. M. (2002) *Mol Cell Endocrinol* **195**, 109-118
24. Bousquet, C., Susini, C., and Melmed, S. (1999) *J Clin Invest* **104**, 1277-1285
25. Frangioni, J. V., Beahm, P. H., Shifrin, V., Jost, C. A., and Neel, B. G. (1992) *Cell* **68**, 545-560
26. Frangioni, J. V., Oda, A., Smith, M., Salzman, E. W., and Neel, B. G. (1993) *Embo J* **12**, 4843-4856
27. Arabaci G., G. X., Beebe KD., Coggeshall KM., Pei D. (1999) *J Am Chem Soc* **121**, 5085-5086
28. Lin, C. F., Chen, C. L., Chang, W. T., Jan, M. S., Hsu, L. J., Wu, R. H., Tang, M. J., Chang, W. C., and Lin, Y. S. (2004) *J Biol Chem* **279**, 40755-40761
29. Perkins, C. L., Fang, G., Kim, C. N., and Bhalla, K. N. (2000) *Cancer Res* **60**, 1645-1653
30. Park, S. J., Wu, C. H., Gordon, J. D., Zhong, X., Emami, A., and Safa, A. R. (2004) *J Biol Chem* **279**, 51057-51067
31. Koeffler, H. P. (2003) *Clin Cancer Res* **9**, 1-9
32. Saez, E., Tontonoz, P., Nelson, M. C., Alvarez, J. G., Ming, U. T., Baird, S. M., Thomazy, V. A., and Evans, R. M. (1998) *Nat Med* **4**, 1058-1061
33. Lefebvre, A. M., Chen, I., Desreumaux, P., Najib, J., Fruchart, J. C., Geboes, K., Briggs, M., Heyman, R., and Auwerx, J. (1998) *Nat Med* **4**, 1053-1057
34. Nikitakis, N. G., Siavash, H., Hebert, C., Reynolds, M. A., Hamburger, A. W., and Sauk, J. J. (2002) *Br J Cancer* **87**, 1396-1403
35. Chen, C. W., Chang, Y. H., Tsi, C. J., and Lin, W. W. (2003) *J Immunol* **171**, 979-988
36. Park, E. J., Park, S. Y., Joe, E. H., and Jou, I. (2003) *J Biol Chem* **278**, 14747-14752
37. Kim, Y., Suh, N., Sporn, M., and Reed, J. C. (2002) *J Biol Chem* **277**, 22320-22329
38. Shiau, C. W., Yang, C. C., Kulp, S. K., Chen, K. F., Chen, C. S., and Huang, J. W. (2005) *Cancer Res* **65**, 1561-1569
39. Haga, S., Terui, K., Zhang, H. Q., Enosawa, S., Ogawa, W., Inoue, H., Okuyama, T., Takeda, K., Akira, S., Ogino, T., Irani, K., and Ozaki, M. (2003) *J Clin Invest* **112**, 989-998
40. Weissenberger, J., Loeffler, S., Kappeler, A., Kopf, M., Lukes, A., Afanasieva, T. A., Aguzzi, A., and Weis, J. (2004) *Oncogene* **23**, 3308-3316
41. Schaefer, L. K., Ren, Z., Fuller, G. N., and Schaefer, T. S. (2002) *Oncogene* **21**,

- 2058-2065
42. Thomas, C. Y., Chouinard, M., Cox, M., Parsons, S., Stallings-Mann, M., Garcia, R., Jove, R., and Wharen, R. (2003) *Int J Cancer* **104**, 19-27
  43. Ostman, A., and Bohmer, F. D. (2001) *Trends Cell Biol* **11**, 258-266
  44. Andersen, J. N., Mortensen, O. H., Peters, G. H., Drake, P. G., Iversen, L. F., Olsen, O. H., Jansen, P. G., Andersen, H. S., Tonks, N. K., and Moller, N. P. (2001) *Mol Cell Biol* **21**, 7117-7136
  45. Hunter, T. (2000) *Cell* **100**, 113-127
  46. Li, B., Chang, C. M., Yuan, M., McKenna, W. G., and Shu, H. K. (2003) *Cancer Res* **63**, 7443-7450
  47. Charest, A., Kheifets, V., Park, J., Lane, K., McMahon, K., Nutt, C. L., and Housman, D. (2003) *Proc Natl Acad Sci U S A* **100**, 916-921
  48. Teixeira, J. E., and Mann, B. J. (2002) *Infect Immun* **70**, 1816-1823
  49. Hsu, S., Schmid, A., Sternfeld, L., Anderie, I., Solis, G., Hofer, H. W., and Schulz, I. (2003) *Cell Signal* **15**, 1149-1156
  50. Palakurthi, S. S., Aktas, H., Grubisich, L. M., Mortensen, R. M., and Halperin, J. A. (2001) *Cancer Res* **61**, 6213-6218

The abbreviations used are: Cyt-c, cytochrome c; Apaf-1, apoptotic protease activating factor-1, FADD, Fas-associated death domain; FLICE, FADD-like IL-1 $\beta$ -converting enzyme; FLIP, FLICE-inhibitory protein, TZD, Thiazolidenediones; PTP, protein tyrosine phosphatase; pY705-STAT3, phospho-tyrosine-705 STAT3; TG, Troglitazone; GW, PPAR $\gamma$  antagonist GW9662; PTPI, PTP inhibitor

### Figure Legends

**Figure 1** DR4/5 expression and TRAIL sensitivity in malignant gliomas. (A) Expression levels of DR4 and DR5 in LN-18, U-87MG and MG-328 cells were analyzed by Western blot. (B) Cells were treated with human rTRAIL (300 ng/ml), and then stained with Annexin V-FITC (Ann) and Propidium Iodide (PI) after 2h-treatment and 24h-treatment. Cells were analyzed by FACS. Presented data is a representative result of LN-18. (C) Cells were treated with human rTRAIL (17.5~300 ng/ml) for 24h, and then stained with Ann and PI. Cells that stained negative for both Ann and PI were defined as viable cells. Data are mean $\pm$ SD of three independent experiments.

**Figure 2** The role of STAT3 in causing resistance to TRAIL in glioma cells. (A, B) STAT3-siRNA (50-600 pmol) or non-silencing siRNA (600 pmol) was transfected to glioma cells (LN-18) with Oligofectamine Reagent. Cells that transfected with Oligofectamine alone were referred to Vehicle. Cells were used for experiments 24h after transfection. (A) Total RNA samples extracted from cells were subjected to real-time quantitative PCR. (B) Protein samples extracted from cells were subjected to Western blot. (C-E) STAT3-siRNA (600 pmol) or non-silencing siRNA (600 pmol) was transfected to glioma cells. Cells that transfected with Oligofectamine alone were referred to Vehicle. (C) Protein samples extracted from cells were subjected to Western blot. (D) Cells were treated with rTRAIL (100 ng/ml) for 24h, and then were stained with Ann and PI. Several groups were cultured for 24h without rTRAIL-treatment. Cells that stained negative for both Ann and PI were defined as viable cells. Data are mean $\pm$ SD of three independent experiments; \*\* refers to statistical significance ( $p < 0.01$ ). (E) The activities of caspase-3, -8, and -9 were measured by enzyme activity assay after 2h of the TRAIL treatment. Non-silencing controls were used for control. The specific activities on each sample were calculated according to the manufacturer's protocol. Data are mean $\pm$ SD of three independent experiments; \*\* refers to statistical significance ( $p < 0.01$ ) compared with each control.

**Figure 3** The synergistic effect of Troglitazone (TG) on TRAIL. (A) Expression of PPAR $\gamma$  in LN-18, U-87MG and MG-328 cells were analyzed by Western blot. (B) Treatment of cells with TG (30  $\mu$ M) for 24h was followed by rTRAIL (100 ng/ml) for 24h. Several groups were cultured for 48h without rTRAIL-treatment. Cells were stained with Ann and PI. Cells that stained negative for both Ann and PI were defined as viable cells. Data are mean $\pm$ SD of three independent experiments; \*\* refers to statistical significance ( $p < 0.01$ ). (C) Protein samples extracted from cells with and without TG-treatment were subjected to Western blot.

**Figure 4** TG activity via PPAR $\gamma$ -dependent and -independent pathways. (A-C) Cells were treated with GW9662 (GW: 20 $\mu$ M) and/or TG (30  $\mu$ M) for 24h. (A) Protein samples extracted from the cells were subjected to Western blot. (B) Treatment of cells with TG and/or GW was followed by rTRAIL (100 ng/ml) treatment for 24h. Cells not treated with TG or GW were used for control. Cells were stained with Ann and PI. Cells that stained negative for both Ann and PI were defined as viable cells. Data are mean $\pm$ SD of three independent experiments; \*\* refers to statistical significance ( $p < 0.01$ ) compared with each control. (C) Treatment of cells with TG and/or GW was followed by rTRAIL (100 ng/ml) treatment for 2h. Cells not treated with TG or GW were used for control. The activities of caspase-3, -8 and -9 were measured by enzyme activity assay. The specific activities on each sample were calculated according to the manufacturer's protocol. Data are mean $\pm$ SD of three independent experiments; \* refers to statistical significance ( $p < 0.05$ ), \*\* refers to statistical significance ( $p < 0.01$ ) compared with each control.

**Figure 5** Expression of PTP1B and SHP-1 after treatment with TG in glioma cells. Protein samples extracted at different time points after treatment with TG (30  $\mu$ M) were subjected to Western blot in which the expressions of pY705-STAT3, PTP1B, and SHP-1 were analyzed.

**Figure 6** The significance of PTP1B in the effect of TG. (A) Cells were treated with TG (30 $\mu$ M) and/or PTP inhibitor (PTPI: 50  $\mu$ M) for 24h. Protein samples extracted from the cells were subjected to Western blot. (B) Cells were treated with TG (30 $\mu$ M) and/or SHP-1 inhibitor (SHPI: 200  $\mu$ M) for 24h. Protein samples extracted from the cells were subjected to Western blot. (C) Treatment of cells with TG and/or PTPI was followed by rTRAIL (100 ng/ml) for 2h. Cells non-treated with TG or PTPI were used for control. The activities of caspase-3, -8, and -9 were measured by enzyme activity assay. The specific activities on each sample were calculated according to the manufacturer's protocol. Data are mean $\pm$ SD of three independent experiments; \*\* refers to statistical significance ( $p < 0.01$ ) compared with each control. (D) STAT3-siRNA (600 pmol) or non-silencing siRNA (600 pmol) was transfected to glioma cells. Cells that transfected with Oligofectamine alone were referred to Vehicle. Cells were used for experiments 24h after transfection. The activities of caspase-3, -8 and -9 were measured similar to Figure 6C. Data are mean $\pm$ SD of three independent experiments; \* refers to statistical significance ( $p < 0.05$ ), \*\* refers to statistical significance ( $p < 0.01$ ) compared with each non-silencing control.

**Figure 7** Synergistic effect of TG on chemotherapeutic drugs. (A-D) U-87MG cells were treated with TG (30 $\mu$ M) and/or a PTP inhibitor (PTPI: 50  $\mu$ M) for 24h. (A, B) Treatment of cells with TG and/or PTPI was followed by treatment with VP16 (A: 0.01-10  $\mu$ M) or Taxol (B: 0.005-5  $\mu$ M) for 48h. Cells not treated with TG or PTPI were used for control. Cells were stained with Ann and PI. Cells that stained negative for both Ann and PI were defined as viable cells. Data are mean $\pm$ SD of three independent experiments; \* refers to statistical significance ( $p < 0.05$ ), \*\* refers to statistical significance ( $p < 0.01$ ) compared with each control. (C, D) Treatment of cells with TG and/or PTPI was followed by treatment with VP16 (C: 10  $\mu$ M) or Taxol (D: 5  $\mu$ M) for 24h. Cells not treated with TG or PTPI were used for control. The activities of caspase-3, -8 and -9 were measured by enzyme activity assay. The specific activities on each

sample were calculated according to the manufacturer's protocol. Data are mean $\pm$ SD of three independent experiments; \* refers to statistical significance ( $p<0.05$ ), \*\* refers to statistical significance ( $p<0.01$ ) compared with each control.

**Figure 8** Schema of TG's synergistic activities on TRAIL, VP16, and Taxol for facilitation of caspase cascade signaling.

Figure 1

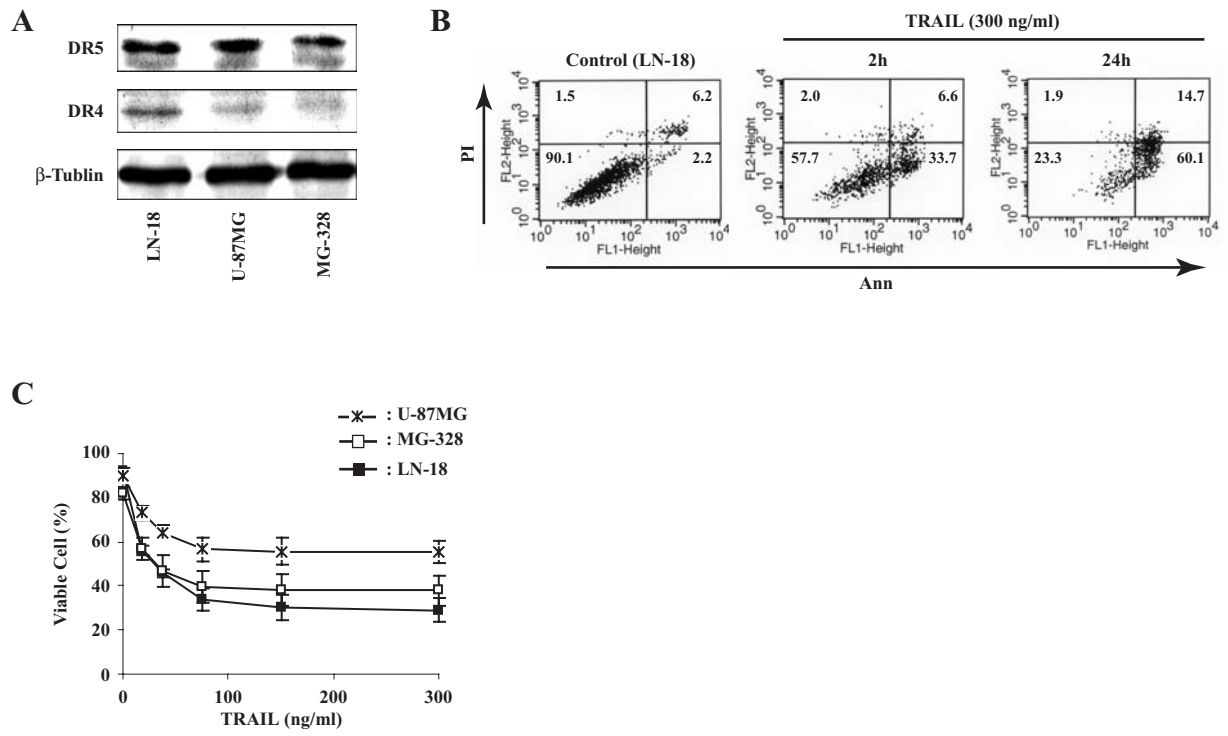


**Figure 2**

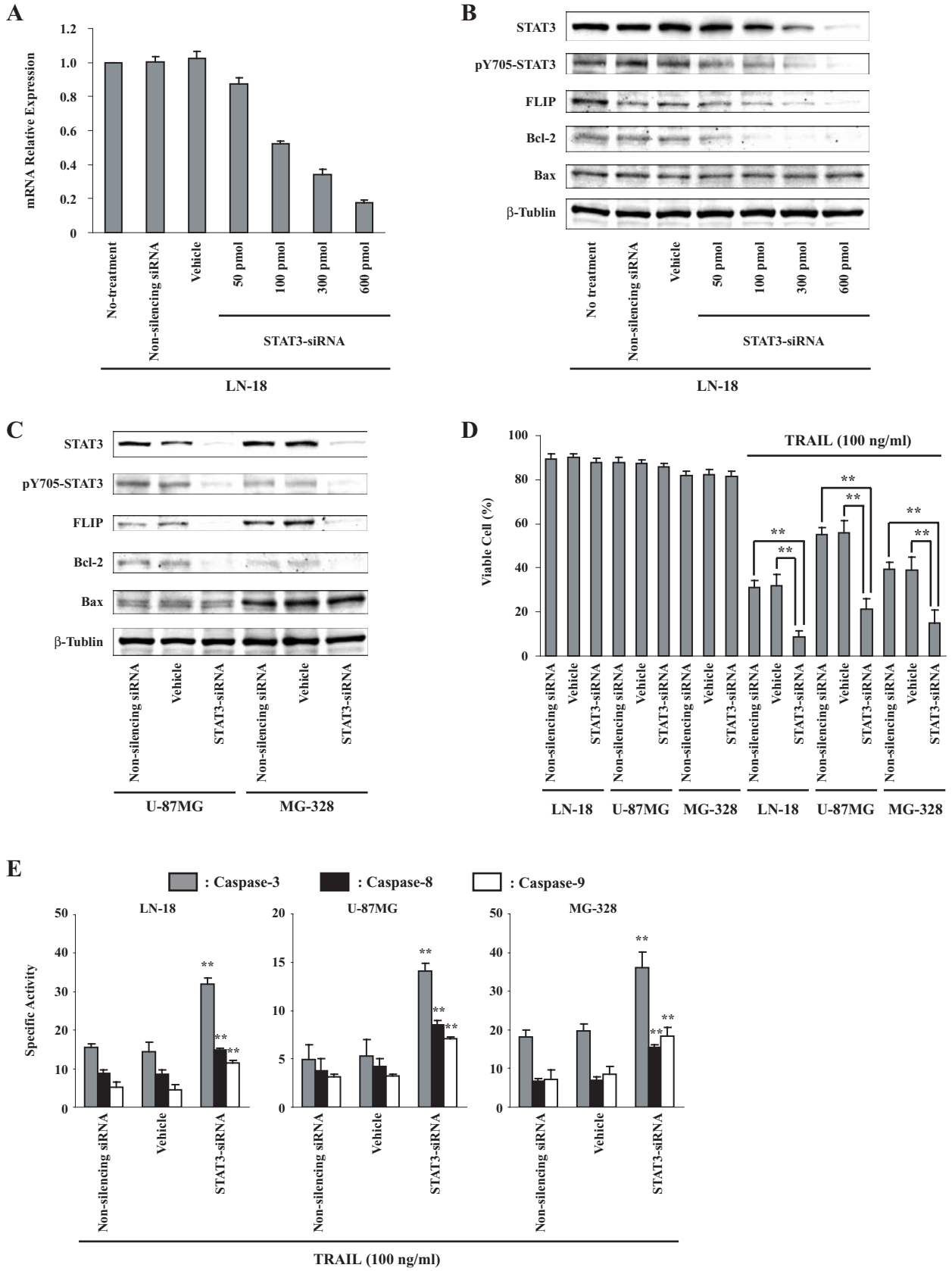
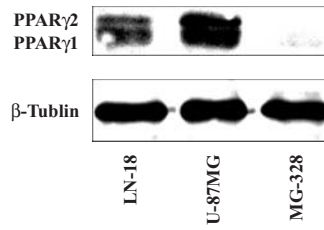
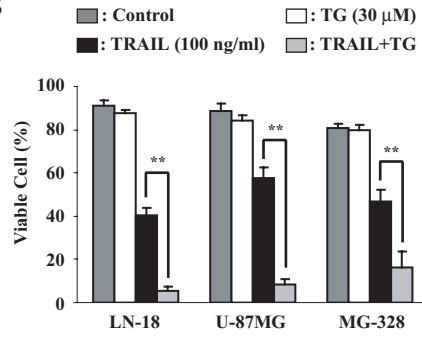


**Figure 3**

**A**



**B**



**C**

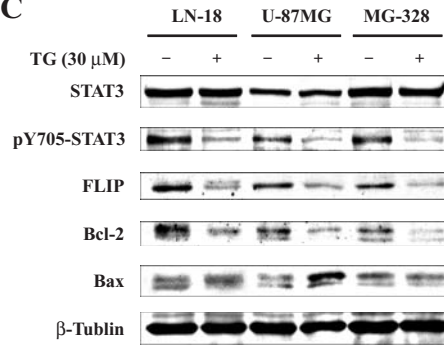


**Figure 4**

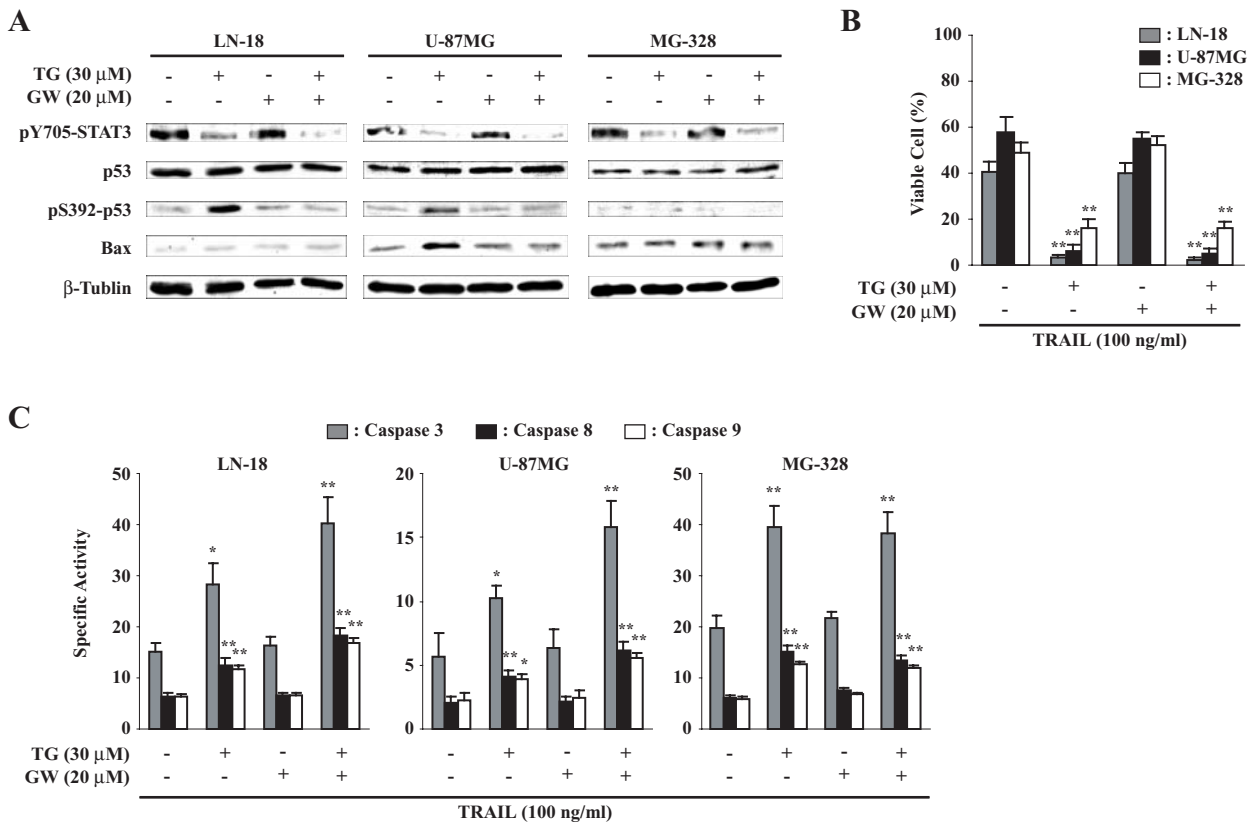


**Figure 5**

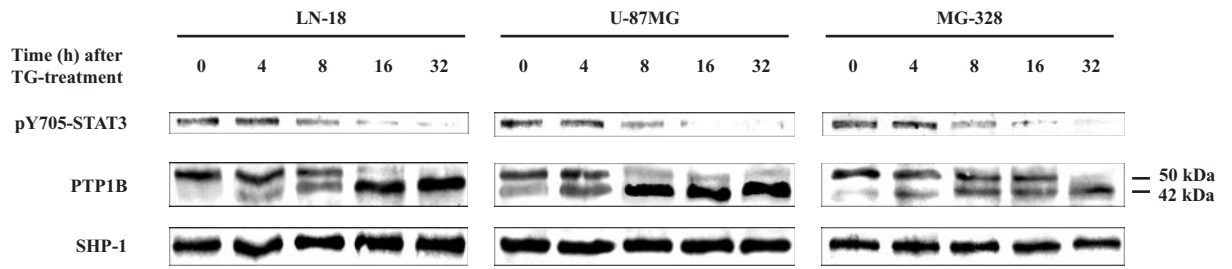


**Figure 6**

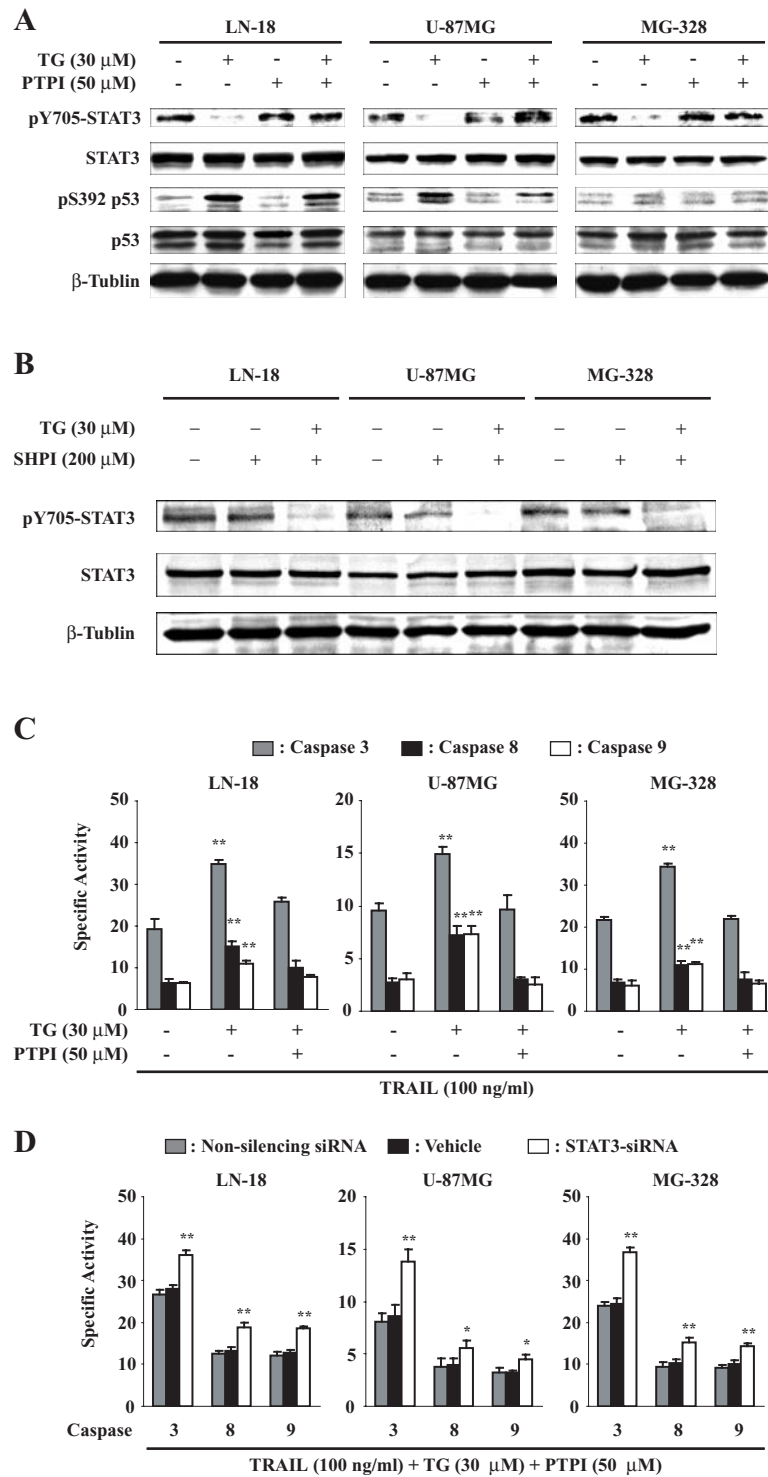


**Figure 7**

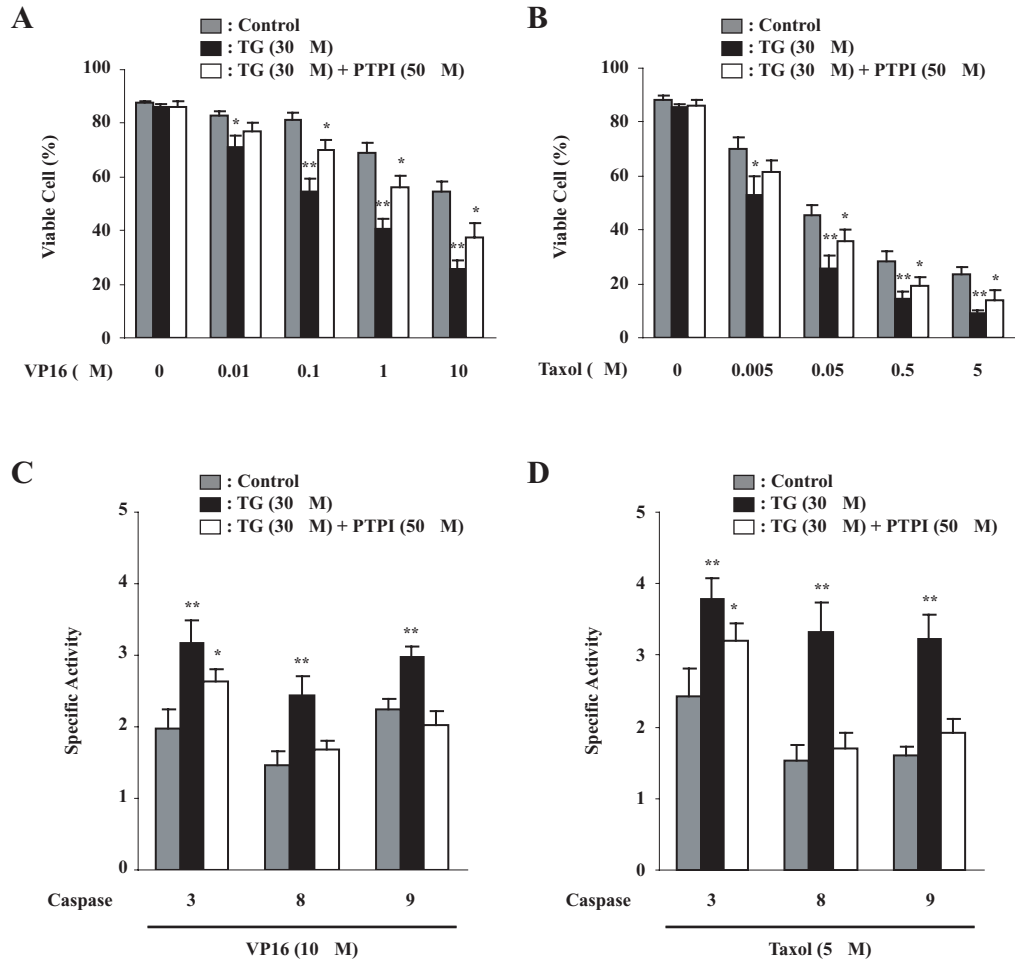


**Figure 8**

